New Analogues of Epiboxidine Incorporating the 4,5-Dihydroisoxazole Nucleus: Synthesis, Binding Affinity at Neuronal Nicotinic Acetylcholine Receptors, and Molecular Modeling Investigations

by **Clelia Dallanoce***[a]), **Pietro Magrone**[a]), **Paola Bazza**[a]), **Giovanni Grazioso**[a]), **Luca Rizzi**[a]), **Loredana Riganti**[b]), **Cecilia Gotti**[b]), **Francesco Clementi**[b]), **Karla Frydenvang**[c]), and **Marco De Amici**[a])

[a]) Istituto di Chimica Farmaceutica e Tossicologica 'Pietro Pratesi', Università degli Studi di Milano, Via Mangiagalli 25, I-20133 Milano (phone: +39-02-50319327; fax: +39-02-50319326; e-mail: clelia.dallanoce@unimi.it)

[b]) CNR, Istituto di Neuroscienze, Farmacologia Cellulare e Molecolare e Dipartimento Farmacologia, Chemioterapia e Tossicologia Medica, Università degli Studi di Milano, Via Vanvitelli 32, I-20129 Milano

[c]) Department of Medicinal Chemistry, Faculty of Pharmaceutical Sciences, University of Copenhagen, Universitetsparken 2, DK-2200 Copenhagen

A group of novel 4,5-dihydro-3-methylisoxazolyl derivatives, structurally related to epiboxidine (= (1*R*,4*S*,6*S*)-6-(3-methylisoxazol-5-yl)-7-azabicyclo[2.2.1]heptane), was prepared *via* 1,3-dipolar cycloaddition of acetonitrile oxide to different olefins. Target compounds **1a** and **1b**, **2a** and **2b**, **3**, **4**, and **5** were tested for affinity at neuronal nicotinic heteromeric ($\alpha4\beta2$) and homomeric ($\alpha7$) acetylcholine receptors. Notably, diastereoisomers **1a** and **1b** were characterized by a massive drop of the affinity at the $\alpha4\beta2$ subtypes (K_i values spanning the range 4.3–126 μM), when compared with that of epiboxidine (K_i = 0.6 nM). Therefore, the replacement of the 3-methylisoxazole ring of epiboxidine with the 4,5-dihydro-3-methylisoxazole nucleus is detrimental for the affinity at $\alpha4\beta2$ receptors. A comparable lack of affinity/selectivity for the two nAChR subtypes under study was evidenced for the remaining epiboxidine-related dihydroisoxazole derivatives **2a** and **2b**, and **3**–**5**. Diastereoisomers **1a** and **1b**, and spirocyclic derivative **3** were docked into molecular models of the receptor subtypes under study, and their binding mode was compared with that of reference ligands endowed with high binding affinity.

Introduction. – Neuronal nicotinic acetylcholine receptors (nAChRs) belong to a heterogeneous family of ligand-operated ion channels differently expressed in the central and peripheral nervous systems [1–3]. The receptors are composed of five separate transmembrane proteins (subunits), each containing a long N-terminal extracellular domain, four membrane spanning α helices (M1–M4), a large cytoplasmatic loop linking M3 and M4 sequences, and a short C-terminal extracellular domain [4]. The resulting transmembrane ion channel is assembled in a pentameric architecture to form a pore which is permeable to cations such as Na^+, K^+, or Ca^{2+}.

Of the 17 different nAChR subunits which have been cloned so far, twelve ($\alpha2$ to $\alpha10$, and $\beta2$ to $\beta4$) were found in the neuronal receptors of vertebrates [5]. Different subunit combinations characterize the nicotinic receptors expressed within the diverse areas of the central nervous system (CNS) [6][7], and affect their biophysical and functional properties, such as ion selectivity, conductance, mean open-channel time, rate of desensitization, as well as the sensitivity to neurotoxins [4]. On the other hand,

ongoing investigations on the pharmacology and neurobiology of CNS nAChRs allowed a better understanding of their involvement in various neuropsychiatric pathologies, such as *Alzheimer*'s and *Parkinson*'s diseases, mild cognitive impairment (MCI), *Tourette*'s syndrome, schizophrenia, depression, anxiety, attention-deficit hyperactivity disorder (ADHD), and nicotine addiction [1].

More than 90% of the heteromeric channels localized in the CNS contain the $\alpha 4$ and $\beta 2$ subunits, whereas the most abundant homomeric channel is the $\alpha 7$ pentamer [3][8]. As a consequence, research efforts have mainly focused on the discovery of selective $\alpha 4\beta 2$ or $\alpha 7$ ligands, to ascertain the physiological and pathophysiological relevance of these receptor subtypes. Even though a large number of nicotinic agonists and noncompetitive antagonists has been reported, very few of them are subtype-selective [9].

However, over recent years, the advancement of potentially useful nAChR-based therapeutics took advantage of the availability of molecular models for the different nicotinic channels and the elaboration of computational protocols capable to quantitatively estimate the binding free energy of selective ligands. Interesting examples of this strategy are represented by a comparative theoretical study performed on a set of selective agonists of both $\alpha 4\beta 2$ and $\alpha 7$ nAChR subtypes [10], and by the results on a new molecular model of the homomeric $\alpha 7$ channel, developed by our research group, coupled with a computational method that allowed us to reliably evaluate the ligand-receptor recognition process of $\alpha 7$ nAChR agonists [11].

As far as the nAChR ligands selectively activating the $\alpha 4\beta 2$ subtype are considered, a significant impulse to their development was given by the discovery of epibatidine (*Fig. 1*), a toxin isolated from the skin of the poisonous Ecuadorian frog *Epipedobates tricolor* [12], which possesses an analgesic potency *ca.* 100 times higher than that of morphine. The potent analgesic activity of epibatidine, which is 30 times higher than that of nicotine, is due to its high affinity for the $\alpha 4\beta 2$ nAChR subtype [13]. Unfortunately, the therapeutic use of epibatidine as an analgesic drug is hampered by its very narrow therapeutic index, due to the inability to discriminate among the different nAChR subtypes [14]. Nonetheless, epibatidine has been used as a lead for the synthesis of analogues provided with an improved pharmacological profile [15]. A number of modifications to the structural elements of epibatidine, *i.e.*, functionalization and enlargement of the bicyclic skeleton, variation of the substituent at the N-atom and/or its position within the bicyclic structure [2][4], replacement of the pyridyl ring with different heteroaryl moieties, has been set forth to yield a variety of novel epibatidine-related compounds. Among them, (±)-epiboxidine (*Fig. 1*), characterized by the presence of a 3-methylisoxazole ring, emerged as a potent nicotinic receptor agonist, tenfold less potent than epibatidine as antinociceptive agent but about 20-fold less toxic [16]. More recently, homo-epiboxidine and a series of epiboxidine homologues were synthesized and tested in binding as well as cultured cells assays [17].

To explore the relevance of the 3-methylisoxazole moiety of epiboxidine in the interaction with nAChRs, we prepared and tested the two stereoisomeric 4,5-dihydro-3-methylisoxazole analogues **1a** and **1b**, and their structurally related tertiary alcohols **2a** and **2b** (*Fig. 1*). Further compounds bearing the 4,5-dihydro-3-methylisoxazole nucleus were investigated, *i.e.*, derivatives **3** and **4** (*Fig. 1*), in which the 7-azabicyclo[2.2.1]heptane system and the 4,5-dihydroisoxazole ring of isomers **1** are

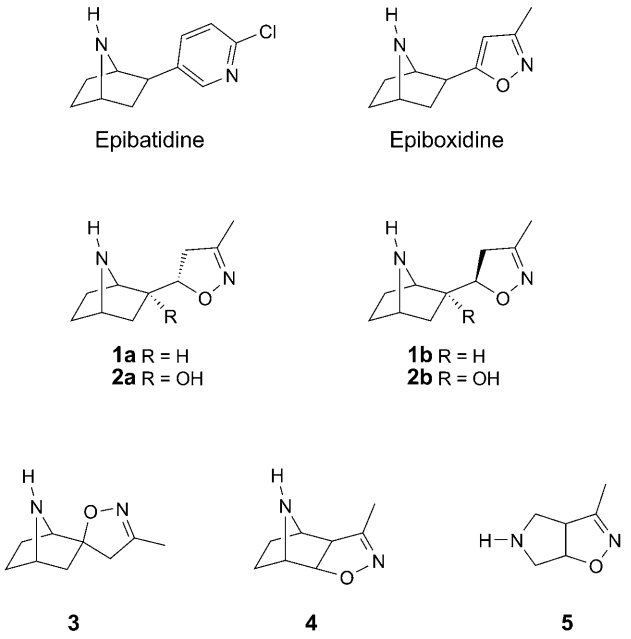

Fig. 1. *Structures of model and target derivatives*

either spiro-linked or fused with the azanorbornane core. Finally, to evaluate the impact of the 7-azabicyclo[2.2.1]heptane skeleton on the affinity profile, we removed the ethylene bridge of **4** to give its simplified analogue **5** *(Fig. 1)*.

This study aimed at further deepening the role exerted by the 4,5-dihydroisoxazole ring in the process of molecular recognition/activation of nAChR subtypes [18][19]. Here, we describe the synthesis of the racemic forms of compounds **1**–**5**, the estimation of their binding affinity at $\alpha4\beta2$ and $\alpha7$ nAChR subtypes, and the qualitative evaluation of the biological results by means of a molecular-modeling analysis.

Results and Discussion. – The synthetic route to the closest analogues of epiboxidine **1a** and **1b**, and **2a** and **2b** is depicted in *Schemes 1* and *2*. Known *tert*-butyl 2-oxo-7-azabicyclo[2.2.1]heptane-7-carboxylate (**6**) [20] was reacted with vinylmagnesium bromide to yield alcohol **7** exclusively. The relative configuration of **7** was assigned on the assumption that the nucleophile approaches from the least hindered *exo*-face. A comparable result was obtained with ketones structurally related to **6** [21]. Alcohol **7** underwent a 1,3-dipolar cycloaddition reaction with *in situ* generated acetonitrile oxide (*Scheme 1*) to give a 2 : 3 mixture (HPLC analysis, 65% overall yield) of stereoisomeric dihydroisoxazoles **9a** and **9b**. 1-Chloroacetaldehyde oxime (**8**) [22], the stable precursor of the 1,3-dipole acetonitrile oxide, was prepared by treating acetaldehyde oxime with benzyl(trimethyl)ammonium tetrachloroiodate (BTMA·ICl_4), according to a recently published procedure [23]. The two cycloadducts were easily separated by column chromatography, and their relative configurations were

unequivocally assigned by an X-ray analysis on isomer **9b**, as detailed in *Fig. 2*. The desired final compounds **2a** and **2b** were obtained as crystalline salts after standard removal of the *N*-Boc protection, followed by treatment with fumaric acid (*Scheme 1*).

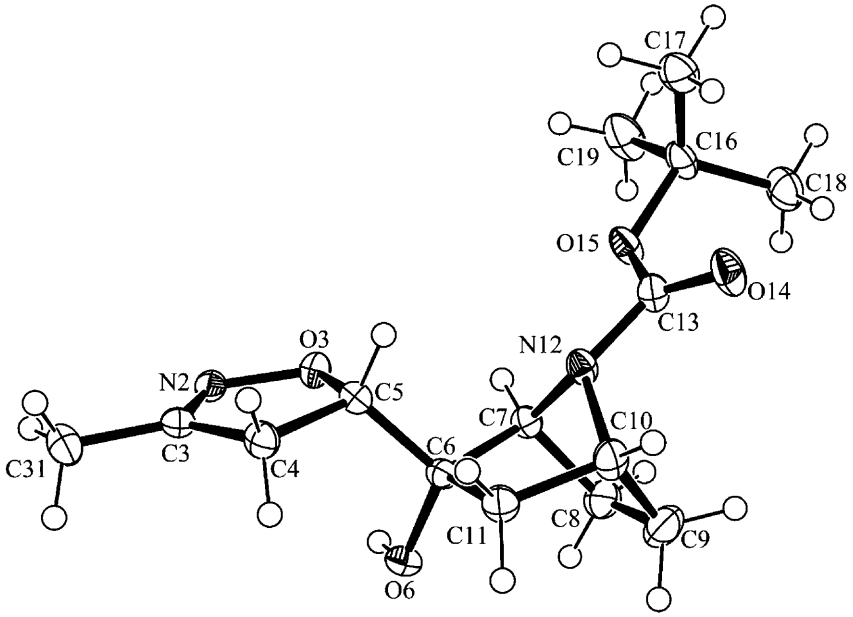

Fig. 2. *Molecular structure* (ORTEP-3) [24] *of compound* **9b** *illustrating the relative configuration.* Displacement ellipsoids of the non-H-atoms are shown at 50% probability level.

Intermediate alcohols **9a** and **9b** were then transformed into the corresponding deoxygenated analogues **11a** and **11b** *via* xanthates **10a** and **10b** [25], respectively, by applying the classic *Barton–McCombie* protocol [26] (*Scheme 2*). The spatial arrangement of the dihydroisoxazole moiety was unaffected by the chemical treatments as testified by the maintenance of the ^{1}H-NMR patterns on passing from **9a** to **11a** and from **9b** to **11b**, respectively. The subsequent preparation of **1a** and **1b** was achieved according to the reactions previously applied to their analogues **2a** and **2b**.

Finally, the 4,5-dihydro-3-methylisoxazolyl derivatives **3**, **4**, and **5** were synthesized according to the three reaction sequences illustrated in *Scheme 3*. Alkene **12** [18], *tert*-butyl 7-azabicyclo[2.2.1]hept-2-ene-7-carboxylate (**13**) [27], and *tert*-butyl 2,5-dihydropyrrole-1-carboxylate **14** [28] were all synthesized according to literature methods. Olefins **12**, **13**, and **14** underwent cycloaddition with acetonitrile oxide to yield the expected cycloadducts **15**, **16**, and **17**, respectively. The reactive olefin **13**, stirred with **8** and Et_3N in CH_2Cl_2 at room temperature, provided **16** in 87% yield. Conversely, the sluggish dipolarophiles **12** and **14** needed to be refluxed in $ClCH_2CH_2Cl$ for a few days with time-to-time addition of further amounts of chloroacetaldehyde oxime and Et_3N. Cycloadducts **15** and **17** were hence isolated in 11 and 27% yields, respectively.

Scheme 1

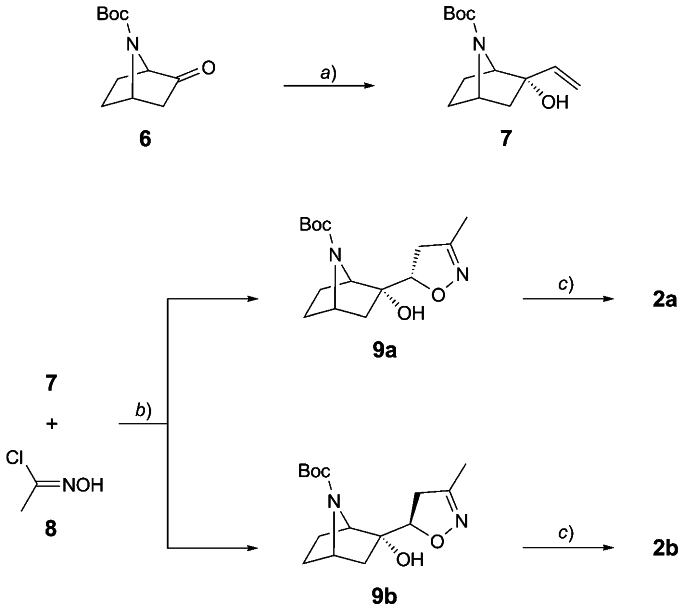

a) Vinylmagnesium bromide (1M in THF), 0°. *b*) Et_3N, CH_2Cl_2. *c*) 30% CF_3COOH, CH_2Cl_2.

As expected, acetonitrile oxide added to the less hindered face of bicyclic olefin **13** yielding the *exo*-cycloadduct **16** exclusively. The observed *exo*-facial selectivity is controlled by the *endo*-pyramidalization of the olefinic H-atoms in the dipolarophile [18][29]. The structural assignment of compound **16** was based on the comparison of relevant ^{1}H-NMR data with those of closely related structural analogues [18]. By taking into account the stereochemical outcome of reactions carried out on olefins structurally related to **12** [18][30], we assigned the *exo*-configuration even to the spirocyclic 4,5-dihydroisoxazole **15**, isolated as single isomer from the cycloaddition step. Sequential treatment of intermediates **15**, **16**, and **17** with CF_3COOH and fumaric acid provided the expected epiboxidine analogues **3**, **4**, and **5**, respectively, as crystalline derivatives.

The target compounds **1a** and **1b**, **2a** and **2b**, **3**, **4**, and **5** were assessed for binding affinity at rat $\alpha4\beta2$ and $\alpha7$ nAChR subtypes, using [^{3}H]epibatidine and [^{125}I]-α-bungarotoxin as radioligands. The K_i values were calculated from the competition curves by means of the LIGAND program [31]. The data reported in the *Table* evidence that the replacement of the 3-methylisoxazole ring of epiboxidine with the 4,5-dihydro-3-methylisoxazole nucleus causes a sharp drop in the affinity at the $\alpha4\beta2$ nAChRs. Indeed, the two stereoisomers **1a** and **1b** show an affinity, at this receptor subtype, four orders of magnitude lower than that reported for epiboxidine (K_i values 9 and 4.3 μM, resp., *vs.* 0.6 nM).

A parallel trend, with a further loss in the binding affinity, was observed on passing to the OH-containing analogues **2a** and **2b** (K_i values 46 and 126 μM, resp.).

Scheme 2

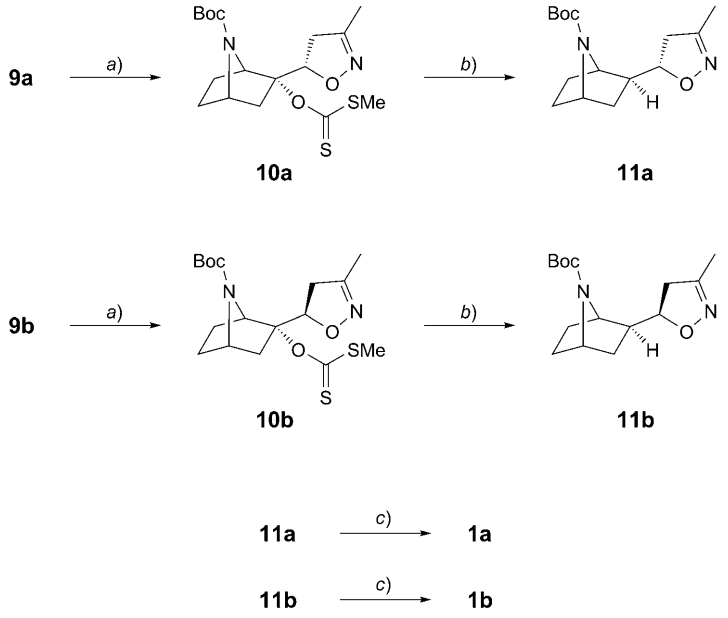

a) NaH, CS_2/MeI, THF, 0°. *b*) 2,2′-Azobis[isobutyronitrile] (AIBN), Bu_3SnH, toluene, reflux. *c*) 30% CF_3COOH, CH_2Cl_2.

Scheme 3

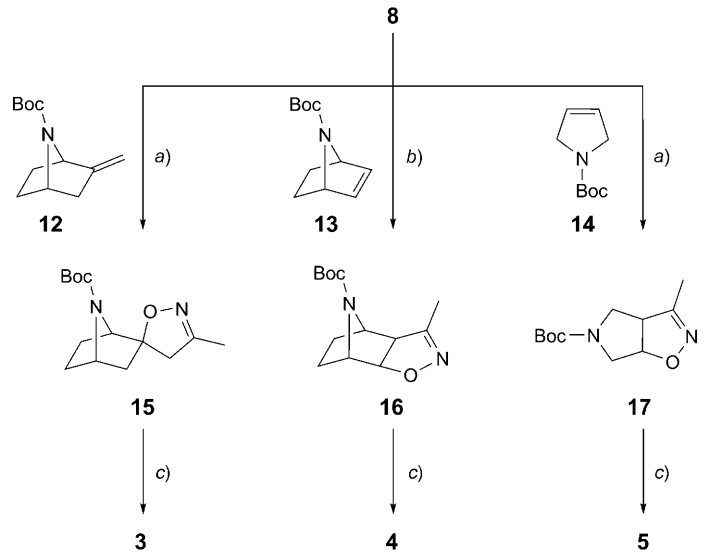

a) Et_3N, CH_2Cl_2. *b*) Et_3N, $ClCH_2CH_2Cl$. *c*) 30% CF_3COOH, CH_2Cl_2.

Table. *Binding Affinities* (K_i [μM]) *of* **1a**, **1b**, **2a**, **2b**, **3**, **4**, *and* **5** *to* $\alpha4\beta2$ *and* $\alpha7$ *nAChR Subtypes*

	$\alpha4\beta2$ [^{3}H]Epibatidine K_i [μM] (% CV)	$\alpha7$ [^{125}I]-α-BgTx K_i [μM] (% CV)
Epibatidine	0.000032	0.0008
α-BgTx	n.d.[a])	0.0009
(±)-Epiboxidine	0.0006[b])	n.d.[c])
1a	9 (16)	32 (42)
1b	4.3 (17)	40 (36)
2a	46 (22)	77(33)
2b	126 (25)	32 (23)
3	4 (19)	15 (19)
4	197 (32)	>500
5	83 (36)	13 (33)

[a]) Not determined. [b]) See [14]. [c]) Unknown value.

Unfortunately, we are not able to comment on the results obtained with the homomeric $\alpha7$ nAChRs, since the data on epiboxidine, to the best of our knowledge, have never been reported. We can only notice that the two couples of structurally related diastereoisomers are provided with a comparable affinity in the micromolar range (K_i values 32–77 μM). Indeed, the overall affinity profile of compounds **1a** and **1b**, and **2a** and **2b** appears to be marginally influenced by the relative configurations at the two stereogenic centers.

On the other hand, either the spiro-linkage or the fusion of the 4,5-dihydro-3-methylisoxazole and the azanorbornane component parts turned out to be unfruitful. Compound **3** is a nonselective ligand with a low binding affinity at both $\alpha4\beta2$ and $\alpha7$ subtypes (K_i values 4 and 15 μM, resp.), whereas derivative **4** is characterized by an affinity at both receptors significantly lower than that displayed by **3** (K_i values 197 and >500 μM, resp.). Finally, removal of the ethylene bridge on passing from derivative **4** to its analogue **5** causes an increase in the distance between the cationic site, *i.e.*, the NH group, and the H-bond acceptor site, *i.e.*, the 4,5-dihydroisoxazole moiety, which increased appreciably the affinity at the $\alpha7$ subtype and reverted the $\alpha4\beta2/\alpha7$ selectivity of the related compounds.

Three selected ligands, *i.e.*, the two isomers **1a** and **1b**, and the spirocyclic derivative **3**, were inspected by means of a molecular-modeling analysis. To this end, we used our model of the $\alpha7$ nAChRs [11] and a recently developed model of the $\alpha4\beta2$ nAChRs [32]. We chose (−)-epibatidine (*Fig. 3*, *c* and *d*) and the yet unknown enantiomer of epiboxidine (*Fig. 3*, *a* and *b*) having the same absolute configuration of (−)-epibatidine as the reference ligands for the $\alpha7$ and $\alpha4\beta2$ receptors, respectively. Similarly, we docked into the models the enantiomers of compounds **1a** and **1b** (*Fig. 3*, *a* and *c*), and **3** (*Fig. 3*, *b* and *d*) whose absolute configuration matches that of (−)-epibatidine.

The high-affinity ligands for the $\alpha4\beta2$ subtype, such as (−)-epibatidine and epiboxidine, give rise to a network of most favorable molecular contacts with the receptor complementary sites, such as *i*) a H-bond involving the NH group of the ligand and the C=O group of the Trp147 residue, *ii*) a network of cation–π interactions with

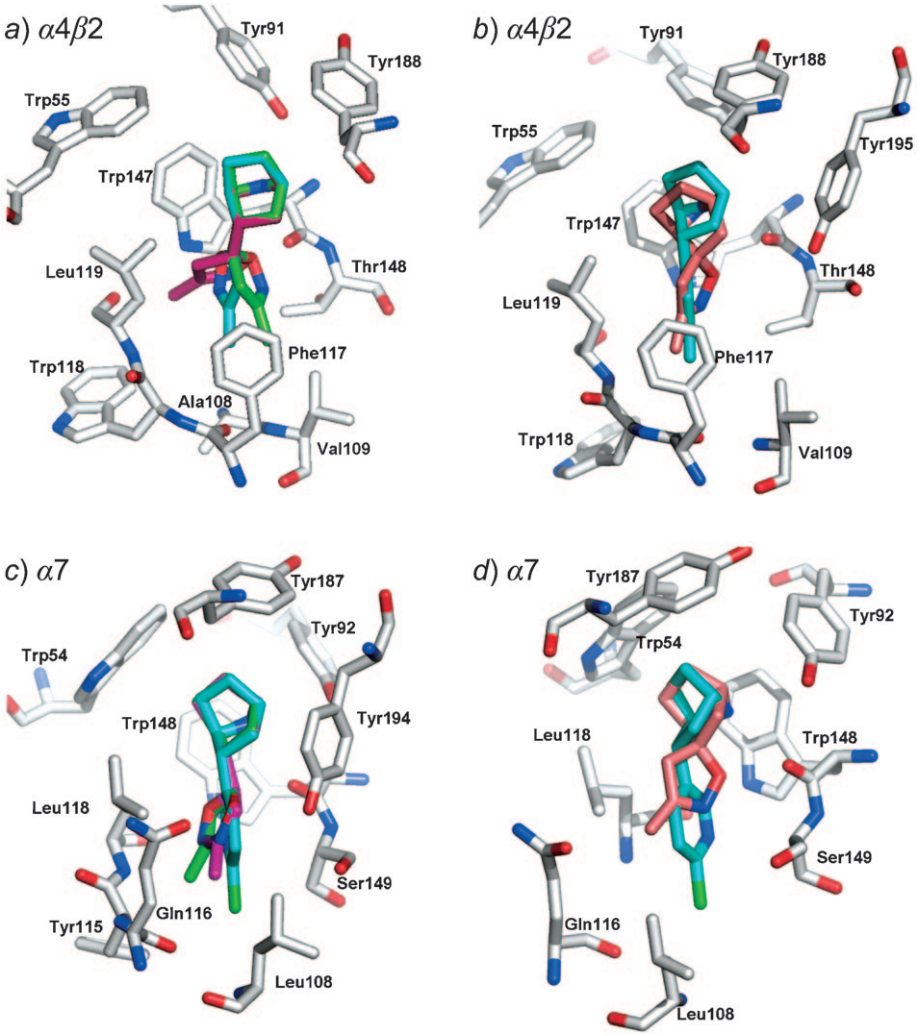

Fig. 3. *Binding of compounds (−)-Epibatidine, Epiboxidine,* **1a**, **1b**, *and* **3** *in the α4β2-nAChR* (*a* and *b*) *and α7-nAChR* (*c* and *d*) *active sites.* Receptor model residues are depicted as stick model, colored according to the atom code (C-atoms in white). Ligands are depicted as stick model, colored according to the atom code: C-atoms in cyan for epiboxidine (*a* and *b*) and (−)-epibatidine (*c* and *d*), in magenta for **1a**, green for **1b**, and pink for **3**.

the so-called 'aromatic box' (Trp55, Trp147, Tyr188, Tyr195), and *iii*) a tight hydrophobic interaction of the ligand heteroaromatic moiety with the Leu119, Phe117, and Val109 residues.

Conversely, a moderate or negligible binding affinity of a ligand is accounted for by a loss in the number and nature of complementary molecular contacts with the receptor and/or by the presence of unfavorable steric interactions. As far as the docking of

isomers **1a** and **1b** into the $\alpha4\beta2$ receptor model is compared with that of epiboxidine, replacement of the heteroaromatic isoxazole group with the flexible 4,5-dihydroisoxazole ring brings about a distortion of the azanorbornane moiety, which is poorly compatible for both isomers **1a** and **1b** with the sterically demanding hydrophobic triad Leu119, Phe117, and Val109 (*Fig. 3*,*a*). In this respect, the docking of both isomers **1a** and **1b** into the $\alpha7$ receptor binding site is further negatively affected, since an even more hindered Leu108 replaces the Val109 residue located on the $\alpha4\beta2$ receptor (*Fig. 3*,*c*).

As far as the binding of compound **3** is considered, the spirocyclic junction engenders a steric clash between the 4,5-dihydroisoxazole moiety and the Leucine residues found in both receptors (Leu119 for the $\alpha4\beta2$ subtype, and Leu118 for the $\alpha7$ subtype), as depicted in *Fig. 3*,*b* and *d*. Therefore, at variance with the reference compounds, the azanorbornane nucleus of **3** is forced to adopt a conformation which considerably hampers the interaction with the above mentioned 'aromatic box' residues. Such a different orientation of ligand **3** in the receptor binding clefts emerges as the leading cause of the drop in affinity at both receptor subtypes.

Conclusions. – In summary, the replacement of the 3-methylisoxazole ring of (±)-epiboxidine with the 4,5-dihydro-3-methylisoxazole nucleus to generate the two diastereoisomers **1a** and **1b** led to a dramatic loss of affinity at $\alpha4\beta2$ nAChRs, thus confirming the essential role played by the heteroaromatic fragment for an effective interaction with the complementary receptor subsites. A molecular-modeling analysis allowed us to clarify that the 4,5-dihydroisoxazole nucleus is precluding a favorable insertion of both diastereoisomers in a hydrophobic cavity of the receptor. Comparable results were also obtained when **1a** and **1b** were docked into a model for the $\alpha7$ nAChRs. More drastic modifications of the epiboxidine molecular skeleton involving insertion of the 4,5-dihydro-3-methylisoxazole moiety, *i.e.*, compounds **3**–**5**, gave also rise to unsatisfactory results, since the three derivatives behaved as low-affinity and nonselective nAChR ligands.

Experimental Part

General. Reagents and solvents for syntheses and crystallizations were reagent-grade and were used without further purification. Solvents for extraction and flash chromatography (FC) were of technical grade and were used without further purification. Solvents for HPLC were purchased from *Sigma-Aldrich*. Compounds **6** [20], **12** [20], **13** [27], and **14** [28] were prepared according to reported procedures. TLC: Al-backed sheets coated with silica gel *60* F_{254}; spots were further evidenced by spraying with a dil. alkaline $KMnO_4$ soln. M.p.: *Büchi B 540* melting-point apparatus; uncorrected. HPLC: *Jasco PU-980* equipped with a UV/VIS detector *Jasco UV-975*, *Lichrosphere Si60* (*Merck*). ^{1}H-NMR Spectra: *Varian Mercury 300* spectrometer, in $CDCl_3$ solns. (unless otherwise indicated); δ in ppm rel. to Me_4Si, *J* in Hz. Microanalyses (C,H,N) of new compounds agreed with the theoretical values within ±0.4%.

Syntheses. tert-*Butyl 2-Ethenyl-2-hydroxy-7-azabicyclo[2.2.1]heptane-7-carboxylate* (**7**). tert-*Butyl 2-oxo-7-azabicyclo[2.2.1]heptane-7-carboxylate* (**6** [20]; 450 mg, 2.13 mmol) was dissolved in anh. THF (20 ml) and cooled to 0°. Vinylmagnesium bromide (1.0M in THF, 4.3 ml, 4.3 mmol) was added dropwise under a flow of anh. N_2, and the mixture was stirred at 0° for 30 min. After addition of a sat. soln. NH_4Cl (20 ml), the mixture was extracted with AcOEt (3 × 10 ml). The collected org. layers were dried (Na_2SO_4), filtered, and evaporated at reduced pressure. The residue was purified by FC (SiO_2; petroleum ether/AcOEt 4 :1) and then crystallized from hexane to afford pure **7** (380 mg, 75%). Colorless prisms.

M.p. 116–117°. R_f (petroleum ether/AcOEt 7:3) 0.64. ^{1}H-NMR: 1.44 (*s*, 9 H); 1.50–1.70 (*m*, 3 H); 1.71–1.89 (*m*, 2 H); 2.04–2.14 (*m*, 1 H); 2.22–2.37 (*m*, 1 H); 3.94 (br. *s*, 1 H); 4.21 (br. *s*, 1 H); 5.04 (*dd*, *J* = 0.7, 10.6, 1 H); 5.22 (*dd*, *J* = 0.7, 16.9, 1 H); 6.12 (*dd*, *J* = 10.6, 16.9, 1 H). Anal. calc. for $C_{13}H_{21}NO_3$ (239.31): C 65.25, H 8.84, N 5.85; found: C 65.49, H 8.61, N 6.02.

1-Chloroacetadehyde Oxime (**8**). Acetaldehyde oxime (670 mg, 11.4 mmol) was dissolved in CH_2Cl_2 (60 ml), and benzyl(trimethyl)ammonium tetrachloroiodate ($BTMA \cdot ICl_4$) (4.77 g, 11.4 mmol) [23] was added. The greenish suspension dissolved within 10 min after vigorous stirring at r.t. to result in a yellow soln. After stirring for additional 30 min, the mixture was diluted with Et_2O (280 ml), and the resulting precipitate was filtered off. Evaporation of the filtrate *in vacuo* gave **8** as a yellow oil, which was used in the following step without further purification.

tert-*Butyl 2-(4,5-Dihydro-3-methylisoxazol-5-yl)-2-hydroxy-7-azabicyclo[2.2.1]heptane-7-carboxylates* (**9a** and **9b**). To a soln. of **7** (1.0 g, 4.18 mmol) in CH_2Cl_2 (33 ml) **8** (600 mg, 6.42 mmol) and Et_3N (900 µl, 6.42 mmol) were added. The mixture was stirred for 3 d at r.t., while further aliquots of **8** (total amount 3.0 g, 32.1 mmol) and Et_3N (total amount 4.5 ml, 32.1 mmol) were added portionwise. The mixture was diluted with AcOEt (30 ml) and sequentially washed with a sat. $NaHCO_3$ soln. (3 × 20 ml), H_2O (1 × 20 ml), and brine (1 × 20 ml). The residual org. layer was dried (Na_2SO_4), filtered, and evaporated at reduced pressure to afford a crude mixture of **9a** and **9b**, which were separated by FC (SiO_2; petroleum ether/AcOEt 4:1). Diastereoisomers **9a** (240 mg) and **9b** (350 mg) were obtained in 48% overall yield. The HPLC analysis of the crude mixture confirmed a **9a**/**9b** ratio of 2:3. The reported relative configurations resulted from the X-ray analysis performed on isomer **9b**, as depicted in *Fig. 2* and described below.

*(1*R**,2*R**,4*S**)*-tert-*Butyl 2-[(5*S**)-4,5-Dihydro-3-methylisoxazol-5-yl]-2-hydroxy-7-azabicyclo[2.2.1]heptane-7-carboxylate* (**9a**). Colorless prisms from $(i\text{-}Pr)_2O$. M.p. 112–114°. R_f (petroleum ether/AcOEt 1:1) 0.43. HPLC (mobile phase: petroleum ether/AcOEt 1:1, flow rate: 0.5 ml/min): t_R 8.84 min. ^{1}H-NMR: 1.43 (*s*, 9 H); 1.52–1.70 (*m*, 4 H); 1.79 (br. *s*, 1 H); 1.99 (*s*, 3 H); 2.14–2.32 (*m*, 2 H); 2.90–3.15 (*m*, 2 H); 3.89 (br. *s*, 1 H); 4.21 (br. *s*, 1 H); 4.59 (*t*, *J* = 9.6, 1 H). Anal. calc. for $C_{15}H_{24}N_2O_4$ (296.36): C 60.79, H 8.16, N 9.45; found: C 60.91, H 7.95, N 9.32.

*(1*R**,2*R**,4*S**)*-tert-*Butyl 2-[(5*R**)-4,5-Dihydro-3-methylisoxazol-5-yl]-2-hydroxy-7-azabicyclo[2.2.1]heptane-7-carboxylate* (**9b**). Colorless prisms from $(i\text{-}Pr)_2O$. M.p. 150–151° R_f (petroleum ether/AcOEt 1:1) 0.26. HPLC (mobile phase: petroleum ether/AcOEt 1:1, flow rate: 0.5 ml/min): t_R 12.59 min. ^{1}H-NMR: 1.44 (*s*, 9 H); 1.50–1.87 (*m*, 6 H); 1.98 (*s*, 3 H); 2.15–2.27 (*m*, 1 H); 2.91 (*d*, *J* = 10.1, 2 H); 4.12–4.24 (*m*, 2 H); 4.68 (*t*, *J* = 10.1, 1 H). Anal. calc. for $C_{15}H_{24}N_2O_4$ (296.36): C 60.79, H 8.16, N 9.45; found: C 60.72, H 8.07, N 9.37.

*(1*R**,2*R**,4*S**)-2-[(5*S**)-3-Methylisoxazol-5-yl]-7-azabicyclo-[2.2.1]heptan-2-ol* (**2a**). Isomer **9a** (142 mg, 0.48 mmol) was dissolved in CH_2Cl_2 (0.8 ml), and CF_3COOH (0.37 ml, 4.80 mmol) was added dropwise. After stirring for 2 h at r.t., the mixture was evaporated *in vacuo*, H_2O (2 ml) was added, and the aq. layer was washed with Et_2O (3 × 3 ml). The residual aq. phase was basified to pH 10 with solid K_2CO_3 and extracted with AcOEt (6 × 3 ml). The collected org. layers were dried (Na_2SO_4), filtered, and evaporated. The free amine was purified by crystallization from Et_2O/CH_2Cl_2 1:1 to afford **2a** (59 mg, 63%). White solid. M.p. 109–111° (dec.). R_f (CH_2Cl_2/MeOH/$NH_3 \cdot H_2O$ 8:2:0.1) 0.55. ^{1}H-NMR: 1.21 (*d*, *J* = 12.8, 1 H); 1.34–1.47 (*m*, 1 H); 1.54–1.64 (*m*, 2 H); 1.81 (br. *s*, 2 H); 1.97 (*s*, 3 H); 2.03 (*dd*, *J* = 5.5, 12.5, 1 H); 2.21–2.32 (*m*, 1 H); 2.94 (*dd*, *J* = 11.0, 17.2, 1 H); 3.07 (*dd*, *J* = 8.8, 17.2, 1 H); 3.32 (*dd*, *J* = 8.8, 11.0, 1 H); 3.66 (br. *s*, 1 H); 4.72 (*dd*, *J* = 8.8, 11.0, 1 H).

To a soln. of **2a** (59 mg, 0.30 mmol) in MeOH (1.5 ml) was added a soln. of fumaric acid (35 mg, 0.30 mmol) in MeOH (1.5 ml). After stirring overnight at r.t., the mixture was concentrated under reduced pressure to afford quantitatively the corresponding fumarate which was crystallized.

2a · $C_4H_4O_4$. Colorless prisms from i-PrOH. M.p. 135–137°. ^{1}H-NMR (CD_3OD): 1.56 (*d*, *J* = 13.9, 1 H); 1.73–1.87 (*m*, 2 H); 1.98 (*s*, 3 H); 2.00–2.12 (*m*, 2 H); 2.44–2.56 (*m*, 1 H); 2.94 (*dd*, *J* = 8.4, 17.9, 1 H); 3.14 (*dd*, *J* = 11.0, 17.9, 1 H); 4.04 (*d*, *J* = 3.7, 1 H); 4.13 (*t*, *J* = 5.1, 1 H); 4.68 (*dd*, *J* = 8.4, 11.0, 1 H); 6.68 (*s*, 2 H). Anal. calc. for $C_{14}H_{20}N_2O_6$ (312.32): C 53.84, H 6.45, N 8.97; found: C 53.68, H 6.59, N 9.11.

*(1*R**,2*R**,4*S**)-2-[(5*R**)-4,5-Dihydro-3-methylisoxazol-5-yl]-7-azabicyclo[2.2.1]heptan-2-ol* (**2b**). Isomer **9b** (180 mg, 0.61 mmol) was reacted with CF_3COOH according to the procedure described for **9a**. The free amine **2b**, obtained in comparable yield (80 mg, 67%), was crystallized from AcOEt to

afford a colorless crystalline compound. M.p. 125–127° (dec.). R_f (CH_2Cl_2/MeOH/$NH_3 \cdot H_2O$ 8:2:0.1) 0.45. ^{1}H-NMR: 1.23 (*d*, *J* = 12.1, 1 H); 1.37–1.49 (*m*, 1 H); 1.52–1.65 (*m*, 2 H); 1.96 (*s*, 3 H); 2.02 (br. *s*, 3 H); 2.18–2.29 (*m*, 1 H); 2.93 (*d*, *J* = 9.3, 2 H); 3.57–3.67 (*m*, 2 H); 4.8 (*t*, *J* = 9.3, 1 H).

The corresponding fumarate was obtained as previously described for **2a**.

2b · *1/2 $C_4H_4O_4$*. Colorless prisms from i-PrOH. M.p. 134–137°. ^{1}H-NMR (CD_3OD): 1.55 (*d*, *J* = 13.5, 1 H); 1.67–1.82 (*m*, 2 H); 1.84–1.95 (*m*, 2 H); 1.97 (*s*, 3 H); 2.34–2.46 (*m*, 1 H); 3.00 (*dd*, *J* = 8.7, 17.4, 1 H); 3.07 (*dd*, *J* = 10.6, 17.4, 1 H); 3.96–4.05 (*m*, 2 H); 4.64 (*dd*, *J* = 8.7, 10.6, 1 H); 6.66 (*s*, 1 H). Anal. calc. for $C_{12}H_{18}N_2O_4$ (254.28): C 56.68, H 7.13, N 11.02; found: C 56.43, H 7.30, N 10.87.

*(1*R**,2*R**,4*S**)*-tert-*Butyl 2-[(5*S**)-4,5-Dihydro-3-methylisoxazol-5-yl]-2-{[(methylsulfanyl)thiocarbonyl]oxy}-7-azabicyclo[2.2.1]heptane-7-carboxylate* (**10a**). A suspension of NaH (110 mg, 4.58 mmol) in dry THF (10 ml) was cooled at 0° under a flow of anh. N_2. To the mixture was added dropwise a soln. of **9a** (466 mg, 1.57 mmol) in dry THF (5 ml). The mixture was stirred at 0° for 10 min, then was allowed to warm to r.t. and stirred for additional 15 min. After cooling again to 0°, CS_2 (775 µl, 12.87 mmol) was added dropwise, and the red-orange soln. was stirred for 30 min at r.t., then cooled to 0°, and MeI (1.56 ml, 25.12 mmol) was added. The mixture was allowed to warm to r.t. and then stirred overnight. A sat. aq. NH_4Cl soln. (20 ml) was added, and the separated aq. layer was extracted with AcOEt (3 × 10 ml). The pooled org. phases were dried (Na_2SO_4), filtered, and evaporated. The residue was purified by FC (SiO_2; petroleum ether/AcOEt 4:1) to afford **10a** as a yellow viscous oil (243 mg, 40%). R_f (petroleum ether/AcOEt 7:3) 0.35. ^{1}H-NMR: 1.45 (*s*, 9 H); 1.52–1.75 (*m*, 4 H); 1.76–1.90 (*m*, 1 H); 1.97 (*s*, 3 H); 2.21–2.34 (*m*, 1 H); 2.52 (*s*, 3 H); 2.93 (*dd*, *J* = 11.5, 17.3, 1 H); 3.05–3.28 (*m*, 1 H); 4.27 (br. *s*, 1 H); 4.81 (br. *s*, 1 H); 5.99 (*t*, *J* = 10.6, 1 H). Anal. calc. for $C_{17}H_{26}N_2O_4S_2$ (386.53): C 52.82, H 6.78, N 7.25; found: C 53.07, H 6.55, N 7.50.

*(1*R**,2*S**,4*S**)*-tert-*Butyl 2-[(5*S**)-4,5-Dihydro-3-methylisoxazol-5-yl]-7-azabicyclo[2.2.1]heptane-7-carboxylate* (**11a**). To a soln. of 2,2′-azobis[isobutyronitrile] (AIBN; 180 mg, 1.10 mmol) in toluene (65 ml) was cautiously added a soln. of BuSnH (2.5 ml, 9.28 mmol) in toluene (40 ml). To the mixture heated at reflux under anh. N_2, a soln. of **10a** (450 mg, 1.16 mmol) in toluene (20 ml) was added dropwise over 20 min. After stirring at reflux for 6 h, the crude mixture was concentrated at reduced pressure, and the residue was submitted to FC (SiO_2; petroleum ether/AcOEt 3:2) to give **11a** (200 mg, 61%). Pale yellow oil. R_f (petroleum ether/AcOEt 1:1) 0.21. ^{1}H-NMR: 1.22–1.36 (*m*, 2 H); 1.44 (*s*, 9 H); 1.64–1.88 (*m*, 4 H); 1.98 (*s*, 3 H); 2.21–2.35 (*m*, 1 H); 2.58 (*dd*, *J* = 8.4, 16.8, 1 H); 3.01 (*dd*, *J* = 9.9, 16.8, 1 H); 4.18 (br. *s*, 1 H); 4.29 (br. *s*, 1 H); 4.32–4.44 (*m*, 1 H). Anal. calc. for $C_{15}H_{24}N_2O_3$ (280.36): C 64.26, H 8.63, N 9.99; found: C 64.43, H 8.55, N 9.72.

*(1*R**,2*S**,4*S**)-2-[(5*S**)-4,5-Dihydro-3-methylisoxazol-5-yl]-7-azabicyclo-[2.2.1]heptane* (**1a**). Intermediate **11a** (190 mg, 0.68 mmol) was reacted with CF_3COOH, according to the protocol applied to **9a**, to afford **1a** (88 mg, 72%). Colorless oil. R_f (CH_2Cl_2/MeOH 4:1) 0.29. ^{1}H-NMR: 1.21–1.69 (*m*, 5 H); 1.75–1.92 (*m*, 1 H); 1.98 (*s*, 3 H); 2.09–2.21 (*m*, 1 H); 2.59 (*dd*, *J* = 8.8, 16.8, 1 H); 2.85–3.08 (*m*, 1 H); 3.45–3.76 (*m*, 2 H); 4.29–4.42 (*m*, 1 H).

The corresponding fumarate was obtained as previously described for **2a**.

1a · *3/4 $C_4H_4O_4$*. Colorless prisms from i-PrOH/MeOH 2:1. M.p. 177–179°. ^{1}H-NMR (CD_3OD): 1.56 (*dd*, *J* = 5.1, 12.8, 1 H); 1.71–1.93 (*m*, 3 H); 1.97 (*s*, 3 H); 2.05–2.32 (*m*, 2 H); 2.40–2.53 (*m*, 1 H); 2.72 (*dd*, *J* = 8.4, 17.2, 1 H); 3.18 (*dd*, *J* = 10.3, 17.2, 1 H); 4.12–4.25 (*m*, 2 H); 4.55–4.78 (*m*, 1 H); 6.67 (*s*, 1.5 H). Anal. calc. for $C_{13}H_{19}N_2O_4$ (267.30): C 56.75, H 6.80, N 9.45; found: C 57.02, H 6.67, N 9.53.

*(1*R**,2*R**,4*S**)-tert-*Butyl 2-[(5*R**)-4,5-Dihydro-3-methyl-4,5-dihydroisoxazol-5-yl]-2-{[(methylsulfanyl)thiocarbonyl]oxy}-7-azabicyclo[2.2.1]heptane-7-carboxylate* (**10b**). Isomer **9b** (410 mg, 1.30 mmol) was reacted according to the protocol reported for **9a**. The crude mixture was purified by FC (SiO_2; petroleum ether/AcOEt 4:1) to afford **10b** (250 mg, 47%). Grey amorphous solid. R_f (petroleum ether/AcOEt 7:3) 0.25. ^{1}H-NMR: 1.45 (*s*, 9 H); 1.50–1.72 (*m*, 4 H); 1.75–1.91 (*m*, 1 H); 1.96 (*s*, 3 H); 2.18–2.38 (*m*, 1 H); 2.51 (*s*, 3 H); 2.95 (*dd*, *J* = 11.4, 17.3, 1 H); 3.22 (*dd*, *J* = 9.5, 17.3, 1 H); 4.22 (br. *s*, 1 H); 5.02 (br. *s*, 1 H); 5.99 (*t*, *J* = 10.4, 1 H). Anal. calc. for $C_{17}H_{26}N_2O_4S_2$ (386.53): C 52.82, H 6.78, N 7.25; found: C 52.94, H 6.66, N 7.43.

*(1*R**,2*S**,4*S**)*-tert-*Butyl 2-[(5*R**)-4,5-Dihydro-3-methylisoxazol-5-yl]-7-azabicyclo[2.2.1]heptane-7-carboxylate* (**11b**). Intermediate **10b** (464 mg, 1.20 mmol) was reacted according to the procedure applied to **11a**. The crude mixture was purified by FC (SiO_2; petroleum ether/AcOEt 3:2) to afford **11b**

as a yellow oil (195 mg, 58%). R_f (petroleum ether/AcOEt 1:1) 0.18. ^{1}H-NMR: 1.17–1.34 (*m*, 2 H); 1.43 (*s*, 9 H); 1.62–1.87 (*m*, 4 H); 1.97 (*s*, 3 H); 2.18–2.33 (*m*, 1 H); 2.58 (*dd*, *J* = 8.8, 16.8, 1 H); 2.98 (*dd*, *J* = 8.4, 16.8, 1 H); 4.05 (br. *s*, 1 H); 4.16 (br. *s*, 1 H); 4.10–4.46 (*m*, 1 H). Anal. calc. for $C_{15}H_{24}N_2O_3$ (280.36): C 64.26, H 8.63, N 9.99; found: C 64.37, H 8.57, N 10.21.

*(1*R**,2*S**,4*S**)-2-[(5*R**)-4,5-Dihydro-3-methylisoxazol-5-yl]-7-azabicyclo[2.2.1]heptane* (**1b**). Intermediate **11b** (196 mg, 0.70 mmol) was reacted with CF_3COOH, according to the protocol reported for **9a** to afford **1b** (82 mg, 65%). Pale yellow oil. R_f (CH_2Cl_2/MeOH 4:1) 0.20. ^{1}H-NMR: 1.27–1.70 (*m*, 5 H); 1.75–1.92 (*m*, 1 H); 1.97 (*s*, 3 H); 2.07–2.21 (*m*, 1 H); 2.58 (*dd*, *J* = 9.1, 16.8, 1 H); 2.89–3.05 (*m*, 1 H); 3.50–3.81 (*m*, 2 H); 4.26–4.43 (*m*, 1 H).

The corresponding fumarate was obtained as previously described for **2a**.

1b·*3/4 $C_4H_4O_4$*. Colorless prisms from i-PrOH/MeOH 2:1. M.p. 162–165° (dec.). ^{1}H-NMR (CD_3OD): 1.56 (*dd*, *J* = 5.1, 13.2, 1 H); 1.69–1.94 (*m*, 3 H); 1.97 (*s*, 3 H); 2.05–2.24 (*m*, 2 H); 2.39–2.52 (*m*, 1 H); 2.72 (*dd*, *J* = 8.3, 17.3, 1 H); 3.19 (*dd*, *J* = 10.6, 17.3, 1 H); 4.12–4.25 (*m*, 2 H); 4.55–4.72 (*m*, 1 H); 6.68 (*s*, 1.5 H). Anal. calc. for $C_{13}H_{19}N_2O_4$ (267.30): C 56.75, H 6.80, N 9.45; found: C 56.57, H 7.05, N 9.61.

tert-*Butyl 3′-Methyl-spiro[7-azabicyclo[2.2.1]heptane-2,5′-[4′*H*]isoxazole]-7-carboxylate* (**15**). To a soln. of **8** (600 mg, 6.42 mmol) in $ClCH_2CH_2Cl$ (30 ml) were sequentially added **12** [20] (837 mg, 4.0 mmol) and Et_3N (900 µl, 6.42 mmol). The mixture was heated at reflux for 4 d, while further amounts of **8** (935 mg, 10 mmol) and Et_3N (1.4 ml, 10 mmol) were added portionwise. After addition of H_2O (20 ml), the separated aq. phase was extracted with CH_2Cl_2 (6 × 20 ml). The collected org. layers were dried (Na_2SO_4), filtered, and evaporated. The crude mixture was purified by FC (SiO_2; petroleum ether/AcOEt 1:1) to provide **15** (117 mg, 11%). Yellow oil. R_f (petroleum ether/AcOEt 3:7) 0.40. ^{1}H-NMR: 1.42 (*s*, 9 H); 1.56 (*d*, *J* = 11.3, 1 H); 1.46–1.82 (*m*, 4 H); 1.97 (*s*, 3 H); 2.32 (*dd*, *J* = 3.5, 12.2, 1 H); 2.78 (*d*, *J* = 18.0, 1 H); 2.99 (*d*, *J* = 18.0, 1 H); 4.12 (br. *s*, 1 H); 4.28 (br. *s*, 1 H). Anal. calc. for $C_{14}H_{22}N_2O_3$ (266.34): C 63.13, H 8.33, N 10.52; found: C 62.91, H 8.54, N 10.43.

*3′-Methyl-spiro[7-azabicyclo[2.2.1]heptane-2,5′-[4′*H*]-isoxazole]* (**3**). Reaction of **15** (110 mg, 0.41 mmol) with CF_3COOH according to the procedure reported for **9a** afforded **3** (55 mg, 80%). Colorless oil. R_f (CH_2Cl_2/MeOH 9:1) 0.32. ^{1}H-NMR: 1.22–1.35 (*m*, 2 H); 1.58–1.70 (*m*, 3 H); 1.97 (*s*, 3 H); 2.07 (*dd*, *J* = 5.1, 13.9, 1 H); 2.87 (*d*, *J* = 17.2, 1 H); 2.97 (*d*, *J* = 17.2, 1 H); 3.44 (*d*, *J* = 4.0, 1 H); 3.66 (*t*, *J* = 4.0, 1 H).

The corresponding fumarate was obtained as previously described for **2a**.

3·*$C_4H_4O_4$*. Colorless prisms from MeOH. M.p. 149–151°. ^{1}H-NMR (CD_3OD): 1.65–1.80 (*m*, 1 H); 1.82–1.94 (*m*, 3 H); 1.98 (*s*, 3 H); 2.08 (*d*, *J* = 14.3, 1 H); 2.35 (*dd*, *J* = 4.4, 14.3, 1 H); 3.12 (*d*, *J* = 17.6, 1 H); 3.27 (*d*, *J* = 17.6, 1 H); 4.04 (br. *s*, 1 H); 4.21 (br. *s*, 1 H); 6.68 (*s*, 2 H). Anal. calc. for $C_{13}H_{18}N_2O_5$ (282.29): C 55.31, H 6.43, N 9.92; found: C 55.53, H 6.18, N 9.70.

tert-*Butyl 5-Methyl-3-oxa-4,10-diazatricyclo[5.2.1.0^{2,6}]dec-4-ene-10-carboxylate* (**16**). Alkene **13** [27] (295 mg, 1.48 mmol) and **8** (187 mg, 2 mmol) were dissolved in CH_2Cl_2 (10 ml). To the stirred soln., Et_3N (280 µl, 2.0 mmol) was added dropwise, and the mixture was further stirred for 4 h at r.t. After pouring into H_2O (10 ml) and the usual workup, the residue was purified by FC (SiO_2; petroleum ether/AcOEt 1:1) to afford **16** (325 mg, 87%) as a crystalline derivative (colorless leaflets from hexane). M.p. 79–80°. R_f (petroleum ether/AcOEt 3:7) 0.54. ^{1}H-NMR: 1.20–1.40 (*m*, 2 H); 1.43 (*s*, 9 H); 1.61 (*s*, 1 H); 1.70–1.88 (*m*, 2 H); 2.00 (*s*, 3 H); 3.23 (*d*, *J* = 8.1, 1 H); 4.35–4.50 (*m*, 1 H); 4.51–4.71 (*m*, 1 H). Anal. calc. for $C_{13}H_{20}N_2O_3$ (252.31): C 61.88, H 7.99, N 11.10; found: C 61.67, H 7.80, N 11.38.

5-Methyl-3-oxa-4,10-diazatricyclo[5.2.1.0^{2,6}]dec-4-ene (**4**). Cycloadduct **16** (280 mg, 1.11 mmol) was reacted with CF_3COOH as previously described to give **4** (137 mg, 81%). Pale yellow oil. R_f (CH_2Cl_2/MeOH 9:1) 0.35. ^{1}H-NMR: 1.10–1.38 (*m*, 2 H); 1.57–1.75 (*m*, 2 H); 1.99 (*s*, 3 H); 3.17 (*d*, *J* = 7.7, 1 H); 3.61 (*d*, *J* = 4.0, 1 H); 3.75 (*d*, *J* = 4.8, 1 H); 4.61 (*d*, *J* = 7.7, 1 H).

The corresponding fumarate was obtained as previously described for **2a**.

4·*$C_4H_4O_4$*. Colorless prisms from AcOEt/MeOH 1:1. M.p. 154–157°. ^{1}H-NMR (CD_3OD): 1.55–1.77 (*m*, 2 H); 1.78–1.93 (*m*, 2 H); 1.99 (*s*, 3 H); 3.62 (*d*, *J* = 8.4, 1 H); 4.26 (*dd*, *J* = 4.2, 15.5, 2 H); 4.80 (*d*, *J* = 8.4, 1 H); 6.69 (*s*, 2 H). Anal. calc. for $C_{12}H_{16}N_2O_5$ (268.27): C 53.73, H 6.01, N 10.44; found: C 55.95, H 6.12, N 10.27.

tert-*Butyl 4,5,6,6a-Tetrahydro-3-methyl-3a*H-*pyrrolo[3,4-*d*]isoxazole-5-carboxylate* (**17**). Alkene **14** [28] (677 mg, 4 mmol) was reacted with **8** according to the protocol for the synthesis of **15**. After the usual workup, the crude mixture was purified by FC (SiO_2; petroleum ether/AcOEt 2 :3) to afford **17** (245 mg, 27%). Yellow oil. R_f (petroleum ether/AcOEt 3 :7) 0.60. ^{1}H-NMR: 1.43 (*s*, 9 H); 2.00 (*s*, 3 H); 3.35–3.58 (*m*, 2 H); 3.70 (*t*, *J* = 8.7, 2 H); 3.82 (*d*, *J* = 12.4, 1 H); 5.09–5.19 (*m*, 1 H). Anal. calc. for $C_{11}H_{18}N_2O_3$ (226.27): C 58.39, H 8.02, N 12.38; found: C 58.60, H 7.98, N 12.13.

*4,5,6,6a-Tetrahydro-3-methyl-3a*H-*pyrrolo[3,4-*d*]isoxazole* (**5**). Reaction of **17** (190 mg, 0.84 mmol) with CF_3COOH produced **5** (95 mg, 90%). Yellow oil. R_f (CH_2Cl_2/MeOH 4 :1) 0.30. ^{1}H-NMR: 1.97 (*s*, 3 H); 2.80 (*dd*, *J* = 3.7, 13.5, 1 H); 2.88 (*dd*, *J* = 7.7, 12.8, 1 H); 3.21 (*d*, *J* = 12.8, 1 H); 3.40 (*d*, *J* = 13.5, 1 H); 3.63 (*t*, *J* = 8.8, 1 H); 5.13 (*dd*, *J* = 3.7, 8.8, 1 H).

The corresponding fumarate was obtained as previously described for **2a**.

5·*3/2 $C_4H_4O_4$*. Colorless prisms from hexane/MeOH 1 :1. M.p. 156–157°. ^{1}H-NMR (CD_3OD): 1.99 (*s*, 3 H); 3.42 (*dd*, *J* = 5.1, 12.8, 2 H); 3.66 (*d*, *J* = 12.8, 2 H); 4.08 (*t*, *J* = 8.8, 1 H); 5.29 (*dd*, *J* = 5.1, 8.8, 1 H); 6.75 (*s*, 3 H). Anal. calc. for $C_{12}H_{16}N_2O_7$ (300.26): C 48.00, H 5.37, N 9.33; found: C 47.75, H 5.51, N 9.12.

*X-Ray Crystallographic Analysis. Structure Determination of Compound (±)-***9b**. Colorless single crystals were obtained from a soln. in $(i\text{-Pr})_2O$. Crystal data: $C_{15}H_{24}N_2O_4$, M_r 296.36, monoclinic, space group $P2_1/c$ (No. 14), $a = 6.0800(7)$ Å, $b = 8.2100(8)$ Å, $c = 31.959(3)$ Å, $\beta = 91.085(10)°$, $V = 1595.0(3)$ Å^3, $Z = 4$, $D_c = 1.234$ Mg m^{-3}, $F(000) = 640$, $\mu(\text{Mo}K_\alpha) = 0.089$ mm^{-1}, $T = 122.0(5)$ K, crystal dimensions $0.1 \times 0.15 \times 0.4$ mm.

Data Collection and Processing. Diffraction data were collected on an *Enraf-Nonius KappaCCD* diffractometer using graphite monochromated MoK_α radiation (λ 0.71073 Å) [33][34]. The reflections were measured in the range $-7 \le h \le 7$, $-10 \le k \le 10$, $-41 \le l \le 41$, ($2.55° < \theta < 27.50°$). Data were reduced using the program EvalCCD [35]. A total of 34141 reflections were averaged according to the point-group symmetry 2/*m* resulting in 3652 unique reflections ($R_{int} = 0.0472$ on F_o^2).

Structure Solution and Refinement. The structure was solved by the direct method using the programme SHELXS97 [36][37] and refined using the programme SHELXL97 [38]. Full-matrix least-squares refinement on F^2 was performed, minimizing $\Sigma w(F_o^2 - F_c^2)^2$, with anisotropic displacement parameters for the non-H-atoms. The positions of the H-atoms were located on intermediate difference electron-density maps. Nearly all H-atoms are included in calculated positions, riding on the parent atoms with fixed isotropic displacement parameters. Only the positions of H-atoms connected to stereogenic C-atoms are refined with fixed isotropic displacement parameters. The refinement (206 parameters, 3652 reflections) converged at $R_F = 0.0360$, *$wR_{F^2} = 0.0920$ for 2833 reflections with* $F_o > 4\sigma(F_o)$; $w = 1/[\sigma^2(F_o^2) + (0.0495P)^2 + 0.3240P]$, where $P = (F_o^2 + 2F_c^2)/3$; $S = 1.052$. In the final difference *Fourier* map, maximum and minimum electron densities were 0.291 and -0.225 e Å^{-3}, resp. Complex atomic scattering factors for neutral atoms were as incorporated in SHELXL97 [38][39].

Further details of crystal structure for compound (±)-**9b** have been deposited with the *Cambridge Crystallographic Data Centre*[1]).

Receptor Binding Assay. Membranes binding of [^{3}H]Epibatidine and [^{125}I]-α-Bungarotoxin. The cortex tissues were dissected, immediately frozen on dry ice and stored at –80° for later use. In each experiment, the cortex tissues from two rats were homogenized in 10 ml of a buffer soln. (50 mM Na_3PO_4, 1M NaCl, 2 mM EDTA, 2 mM EGTA, and 2 mM PMSF, pH 7.4) using a potter homogenizer; the homogenates were then diluted and centrifuged at 60,000*g* for 1.5 h. The total membrane homogenization, dilution, and centrifugation procedures were performed twice, then the pellets were collected, rapidly rinsed with a buffer soln. (50 mM *Tris*·HCl, 120 mM NaCl, 5 mM KCl, 1 mM $MgCl_2$, 2.5 mM $CaCl_2$, and 2 mM PMSF, pH 7), and resuspended in the same buffer containing a mixture of 20 μg/ml of each of the following protease inhibitors: leupeptin, bestatin, pepstatin A, and aprotinin.

[^{3}H]Epibatidine Binding. (±)-[^{3}H]Epibatidine with a specific activity of 56–60 Ci/mmol was purchased from *Perkin-Elmer* (Boston, MA); the nonradioactive α-bungarotoxin, nicotine, and epibatidine were purchased from *Sigma*. It has previously been reported that [^{3}H]epibatidine also binds

---

[1]) CCDC-668587 contains the supplementary crystallographic data for this work. These data can be obtained free of charge *via* www.ccdc.cam.ac.uk/data_request/cif.

to α-bungarotoxin-binding receptors with nM affinity [14b]. To prevent the binding of [^{3}H]epibatidine to the α-bungarotoxin-binding receptors, the membrane homogenates were preincubated with 2 μM α-bungarotoxin and then with [^{3}H]epibatidine. The saturation experiments were performed by incubating aliquots of cortex membrane homogenates with 0.01–2.5 nM (±)-[^{3}H]epibatidine overnight at 4°. Nonspecific binding was determined in parallel by means of incubation in the presence of 100 nM unlabelled epibatidine. At the end of the incubation, the samples were filtered on a GFC filter soaked in 0.5% polyethylenimine and washed with 15 ml of a buffer soln. (10 mM Na_3PO_4, 50 mM NaCl, pH 7.4), and the filters were counted in a β counter.

[^{125}I]-α-Bungarotoxin Binding. The saturation binding experiments were performed using aliquots of cortex membrane homogenates incubated overnight with concentrations ranging from 0.1–10 nM of [^{125}I]-α-bungarotoxin (specific activity 200–213 Ci/mmol, *Amersham*) at r.t. Nonspecific binding was determined in parallel by means of incubation in the presence of 1 μM unlabelled α-bungarotoxin. After incubation, the samples were filtered as described above, and the bound radioactivity was directly counted in a γ counter.

nACh Receptor Affinity of Derivatives **1a** *and* **1b**, **2a** *and* **2b**, *and* **3**–**5**. The inhibition of radioligand binding by epibatidine, nicotine, and the test compounds was measured by preincubating cortex homogenates with increasing doses (10 pM–10 mM) of the reference nicotinic agonists, epibatidine or nicotine, and the drug to be tested for 30 min at r.t., followed by overnight incubation with a final concentration of 0.075 nM [^{3}H]epibatidine or 1 nM [^{125}I]- α-bungarotoxin at the same temp. as those used for the saturation experiments. These ligand concentrations were used for the competition binding experiments, because they are within the range of the K_D values of the ligands for the two different classes of nAChRs. For each compound, the experimental data obtained from the three saturation and three competition binding experiments were analyzed by means of a nonlinear least-square procedure using the LIGAND program as described by *Munson* and *Rodbard* [31]. The binding parameters were calculated by simultaneously fitting three independent saturation experiments, and the K_i values were determined by fitting the data of three independent competition experiments. The errors in the K_D and K_i values of the simultaneous fits were calculated using the LIGAND software, and expressed as percentage coefficients of variation (% CV). When final compound concentrations up to 500 μM did not inhibit radioligand binding, the K_i value was defined as being >500 μM based on the *Cheng* and *Prusoff*'s equation [40].

Molecular Modeling. Ligands docked into the receptor binding clefts were built by Sybyl 8.0 (*Tripos Inc.*, 1699 South Hanley Rd., St. Louis, MO 63144) and preliminarily minimized at the HF/6-31g* level as implemented in Gaussian 03 [41]. The amino groups were considered in the ionized form to better simulate the physiological conditions.

We made use of our recently published α7 nAChR [11] molecular model and of a model of $\alpha4\beta2$ nAChRs elaborated at the University of Florence [32]. Docking experiments of the tested ligands were performed by means of the program GOLD 3.2 [42]; the goldscore fitness function, and the distribution of torsion angles were chosen as indicators of the quality of the docking results. *Van der Waals* and H-bonding radii were set at 4.0 and 3.0 Å, resp., while genetic algorithm parameters were kept at the default value. The resulting complexes were then optimized by means of a molecular-mechanics method implemented in the Sybyl 8.0 software. Figures were acquired by the PyMOL software [43].

This research was financially supported by the Italian *FIRB* grant # RBNE03FH5Y002, the *PRIN* grant # 2005054943 (*F. C.*, *C. G.*, and *M. D. A.*), and the *Fondazione Cariplo* grant # 2006/0882 (*F. C.* and *M. D. A.*). We are indebted to Prof. *Paola Gratteri* and co-workers, University of Florence, for the availability of their recently developed model of nicotinic $\alpha4\beta2$ receptors. The authors wish to thank Mr. *F. Hansen*, Center for Crystallographic Studies, University of Copenhagen, for the technical assistance with the X-ray data collection, and Dr. *Maria De Mieri* for her contribution to the synthetic organic chemistry section.

REFERENCES

[1] A. Singh, A. Potter, P. Newhouse, *IDrugs* **2004**, *7*, 1096.
[2] A. A. Jensen, B. Frølund, T. Liljefors, P. Krogsgaard-Larsen, *J. Med. Chem.* **2005**, *48*, 4705.
[3] M. N. Romanelli, P. Gratteri, L. Guandalini, E. Martini, C. Bonaccini, F. Gualtieri, *ChemMedChem* **2007**, *2*, 746.
[4] M. N. Romanelli, F. Gualtieri, *Med. Chem. Rev.* **2003**, *23*, 393, and refs. cit. therein.
[5] J. Lindstrom, 'The Structure of Neuronal Nicotinic Receptors', in 'Handbook of Experimental Pharmacology: Neuronal Nicotinic Receptors', Eds. F. Clementi, C. Gotti, D. Fornasari, Springer-Verlag, Berlin, 2000, p. 101.
[6] S. N. Millar, *Biochem. Soc. Trans.* **2003**, *31*, 869.
[7] C. Gotti, M. Zoli, F. Clementi, *Trends Pharmacol. Sci.* **2006**, *27*, 482.
[8] J. D. Schmitt, *Curr. Med. Chem.* **2000**, *7*, 749.
[9] G. K. Lloyd, M. Williams, *J. Pharmacol. Exp. Ther.* **2000**, *292*, 461.
[10] X. Huang, F. Zheng, X. Chen, P. A. Crooks, L. P. Dwoskin, C.-G. Zhan, *J. Med. Chem.* **2006**, *49*, 7661.
[11] G. Grazioso, A. Cavalli, M. De Amici, M. Recanatini, C. De Micheli, *J. Comput. Chem.* **2008**, *29*, **2593**.
[12] T. F. Spande, H. M. Garraffo, M. W. Edwards, H. J. C. Yeh, L. Pannell, J. W. Daly, *J. Am. Chem. Soc.* **1992**, *114*, 3475.
[13] T. C. Li, C. G. Qian, J. Eckman, D. F. Huang, T. Y. Shen, *Bioorg. Med. Chem. Lett.* **1993**, *3*, 2759.
[14] a) J. P. Sullivan, A. W. Bannon, *CNS Drug Rev.* **1996**, *2*, 21; b) V. Gerzanich, X. Peng, F. Wang, G. Wells, R. Anand, S. Fletcher, J. Lindstrom, *Mol. Pharmacol.* **1995**, *48*, 774; c) J. P. Sullivan, M. W. Decker, J. D. Brioni, D. L. Donnelly-Roberts, D. A. Anderson, A. W. Bannon, C. H. Kang, P. Adams, M. Piattoni-Kaplan, M. J. Buckley, M. Gopalakrishnan, M. Williams, S. P. Arneric, *J. Pharmacol. Exp. Ther.* **1994**, *271*, 624.
[15] J. E. Tønder, P. H. Olesen, *Curr. Med. Chem.* **2001**, *8*, 651, and refs. cit. therein; Z. L. Wei, Y. Xiao, H. Yuan, M. Baydyuk, P. A. Petukhov, J. L. Musachio, K. J. Kellar, A. P. Kozikowski, *J. Med. Chem.* **2005**, *48*, 1721; J. W. Daly, *J. Med. Chem.* **2003**, *46*, 445, and refs. cit. therein.
[16] B. Badio, H. M. Garraffo, C. V. Plummer, W. L. Padgett, J. W. Daly, *Eur. J. Pharmacol.* **1997**, *321*, 189.
[17] J. Cheng, S. Izenwasser, C. Zhang, S. Zhang, D. Wade, M. L. Trudell, *Bioorg. Med. Chem. Lett.* **2004**, *14*, 1775; R. W. Fitch, X.-F. Pei, Y. Kaneko, T. Gupta, D. Shi, I. Federova, J. W. Daly, *Bioorg. Med. Chem.* **2004**, *12*, 179.
[18] C. Dallanoce, P. Bazza, G. Grazioso, M. De Amici, C. Gotti, L. Riganti, F. Clementi, C. De Micheli, *Eur. J. Org. Chem.* **2006**, 3746.
[19] C. De Micheli, M. De Amici, C. Dallanoce, F. Clementi, C. Gotti, PCT Int. Appl. WO 2008000469, 2008.
[20] C. Zhang, M. L. Trudell, *J. Org. Chem.* **1996**, *61*, 7189.
[21] P. Sundararaman, W. Herz, *J. Org. Chem.* **1977**, *42*, 813; G. Rüedi, D. N. Laikov, H. J. Hansen, *Helv. Chim. Acta* **2004**, *87*, 1990.
[22] J. C. Zhang, D. P. Curran, *J. Chem. Soc., Perkin Trans. 1* **1991**, 2627.
[23] S. Kanemasa, H. Matsuda, A. Kamimura, T. Kakinami, *Tetrahedron* **2000**, *56*, 1057.
[24] L. J. Farrugia, ORTEP-3 for Windows, *J. Appl. Crystallogr.* **1997**, *30*, 565.
[25] R. M. Williams, J. Cao, H. Tsujishima, R. J. Cox, *J. Am. Chem. Soc.* **2003**, *125*, 12172; M. G. Banwell, A. J. Edwards, G. J. Harfoot, K. A. Jolliffe, *Tetrahedron* **2004**, *60*, 535.
[26] W. Hartwing, *Tetrahedron* **1983**, *39*, 2609.
[27] F. I. Carroll, F. Liang, H. A. Navarro, L. E. Brieaddy, P. Abraham, M. I. Damaj, B. R. Martin, *J. Med. Chem.* **2001**, *44*, 2229.
[28] S. Brandänge, B. Rodriguez, *Synthesis* **1988**, 347; P. Conti, C. Dallanoce, M. De Amici, C. De Micheli, R. Fruttero, *Tetrahedron* **1999**, *55*, 5623.
[29] C. De Micheli, R. Gandolfi, R. Oberti, *J. Org. Chem.* **1980**, *45*, 1209; R. Gandolfi, G. Tonoletti, A. Rastelli, M. Bagatti, *J. Org. Chem.* **1993**, *58*, 6038.

[30] D. P. Curran, *J. Am. Chem. Soc.* **1983**, *105*, 5826; H. C. Brown, W. J. Hammar, J. H. Kawakami, I. Rothberg, D. L. Vander Jagt, *J. Am. Chem. Soc.* **1967**, *89*, 6381.
[31] P. J. Munson, D. Rodbard, *Anal. Biochem.* **1980**, *107*, 220.
[32] P. Gratteri (University of Florence), personal communication, 2008.
[33] COLLECT, *B. V. Nonius*, Delft, 1999.
[34] A. J. M. Duisenberg, *J. Appl. Crystallogr.* **1992**, *25*, 92.
[35] A. J. M. Duisenberg, EvalCCD, Ph.D. Thesis, University of Utrecht, Utrecht, 1998.
[36] G. M. Sheldrick, SHELXS97, Program for the Solution of Crystal Structure, University of Göttingen, Göttingen, 1997.
[37] G. M. Sheldrick, *Acta Crystallogr., Sect. A* **1990**, *46*, 467.
[38] G. M. Sheldrick, SHELXL97, Program for the Refinement of Crystal Structures, University of Göttingen, Göttingen, 1997.
[39] A. J. C. Wilson, in 'International Tables for Crystallography', Kluwer Academic Publishers, Dordrecht, 1995, Vol. C, Tables 4.2.6.8 and 6.1.1.4.
[40] Y.-C. Cheng, W. H. Prusoff, *Biochem. Pharmacol.* **1973**, *22*, 3099.
[41] M. J. Frisch, G. W. Trucks, H. B. Schlegel, G. E. Scuseria, M. A. Robb, J. R. Cheeseman, J. A. Montgomery Jr., T. Vreven, K. N. Kudin, J. C. Burant, J. M. Millam, S. S. Iyengar, J. Tomasi, V. Barone, B. Mennucci, M. Cossi, G. Scalmani, N. Rega, G. A. Petersson, H. Nakatsuji, M. Hada, M. Ehara, K. Toyota, R. Fukuda, J. Hasegawa, M. Ishida, T. Nakajima, Y. Honda, O. Kitao, H. Nakai, M. Klene, X. Li, J. E. Knox, H. P. Hratchian, J. B. Cross, V. Bakken, C. Adamo, J. Jaramillo, R. Gomperts, R. E. Stratmann, O. Yazyev, A. J. Austin, R. Cammi, C. Pomelli, J. W. Ochterski, P. Y. Ayala, K. Morokuma, G. A. Voth, P. Salvador, J. J. Dannenberg, V. G. Zakrzewski, S. Dapprich, A. D. Daniels, M. C. Strain, O. Farkas, D. K. Malick, A. D. Rabuck, K. Raghavachari, J. B. Foresman, J. V. Ortiz, Q. Cui, S. Baboul, J. Clifford, B. B. Cioslowski, G. Stefanov, A. Liu, P. Liashenko, I. Piskorz, A. G. Komaromi, R. L. Martin, D. J. Fox, T. Keith, M. A. Al-Laham, C. Y. Peng, A. Nanayakkara, M. Challacombe, P. M. W. Gill, B. Johnson, W. Chen, M. W. Wong, C. Gonzalez, J. A. Pople, Gaussian 03, Revision B.04, *Gaussian, Inc.*, Wallingford CT, 2004.
[42] Gold v. 3.2, Cambridge Crystallographic Data Centre, Cambridge, UK.
[43] W. L. DeLano, The PyMOL Molecular Graphics System, *DeLano Scientific*, Palo Alto, 2002; http://www.pymol.org.

Received February 20, 2008